COMPACT BANDPASS FILTER WITH WIDE STOP-BAND USING RECTANGULAR STRIPS, ASYMMETRIC OPEN-STUBS AND L SLOT LINES

Fang Xu[1], Mi Xiao[1, *], Zongjie Wang[1], Jiayang Cui[1], Zhe Zhu[1], Mu Ju[2], and Jizong Duan[1]

[1]School of Electronic Information Engineering, Tianjin University, Tianjin 300072, China

[2]Southeast University, Nanjing 211100, China

Abstract—A novel slot-line filter with stop-band up to 30 GHz is proposed in this paper, and the theoretical analysis is illustrated in detail. This filter is designed on a Rogers RT/duroid 5870 substrate. The rectangular micro-strips can generate transmission zero to give a great suppression for the spurious response around $5f_0$ while the L slot lines can create transmission zeros to suppress the spurious response around $7f_0$, $9f_0$ and $11f_0$. f_0 is 2.43 GHz in this paper and represents the center frequency of the main passband. The compact size of this novel filter is $23.7\,\mathrm{mm} * 14.725\,\mathrm{mm}$ ($0.152\lambda * 0.103\lambda$ (λ is the working wavelength of this filter)). Besides, the external quality factor of this filter can be as high as about 29.6. To demonstrate the transmission function, the compact filter has been fabricated and the measured results show the feasibility of this structure.

1. INTRODUCTION

With the development of modern communication technology, WiFi and blue-tooth applications require small-sized filters with wide stop-band. Microstrip bandpass filters with low insertion loss, compact size and high Q play more and more important roles in mobile communication systems and radio frequency (RF) front/end of the wireless communication systems [1–4]. Planar bandpass filters (BPFs) having compact size and a very wide stopband are very popular to implement the radio frequency (RF) front end in microwave communication systems [5]. As is konwn to us that the micro-strip filter

coupled with coplanar waveguide (CPW) resonators can reach good performance in reduced size. The CPW structure has been proposed in the literature [6]. As is known to us that although the filter based on half-wave coplanar waveguide resonator is widely used, there are spurious responses around nf_0 [7] (f_0 is the center frequency of the passband). The CPW filter was implemented on the basis of end-coupled half wavelength CPW resonator [8, 9]. In literature [5], the CPW in-line quarter-wavelength stepped-impedance resonator band-pass filter is presented to suppress the spurious responses around $2nf_0$. In 2006, the theory was proposed that spurious passbands around $(2n - 1)f_0$ ($n = 1, 2, 3$) exist for the filter based on quarter-wavelength CPW resonator [10]. In order to suppress the spurious passbands, many methods has been presented such as methods using the stepped-impedance resonators and grounded-step-impedance resonators [11, 18, 20, 23, 25, 26], fractal-shaped micro-strip [12], multi-order resonator [13], T-stub/DGS [14], antisymmetric modied anti-parallel coupled-lines [15, 19, 21], branch stubs co-via structure [22], DGS and Spur-line Coupling Structures [24], etc.. However, the size of structures above is not small enough and the higher frequency spurious passbands can not also be suppressed efficiently [10–15, 18–26]. Open-stub and air-bridge have been introduced to create transmission zeros around $3f_0$ and $5f_0$ in a compact filter [16]. While higher order spurious responses are still hard to be suppressed in a miniaturization design.

In this paper, a compact filter with the size of $24\,\text{mm} * 14.725\,\text{mm}$ is proposed. As shown in Fig. 6, the asymmetric open-stubs and rectangular micro-strips are introduced to generate transmission zeros around $3f_0$ and $5f_0$ (f_0 is $2.43\,\text{GHz}$), respectively, while L slot lines can give a great suppression to the spurious response around $7f_0$, $9f_0$ and $11f_0$. The proposed slot-line band-pass filter has the merits of a wide stop-band up to $30\,\text{GHz}$ and a 3-dB bandwidth of $123\,\text{MHz}$.

2. THE FILTER DESIGN

2.1. The Coupling Theory of the Spiral Resonators

Resonators are the key components of a microwave filter so that it is important to study the resonators for the filter design. Fig. 1(a) shows the prototype of the spiral resonators used in novel filter in this paper. Two spiral resonators can generate two resonant points respectively and transmit signal through coupling. The coupling methods can be classified as electric coupling and magnetic coupling. The equivalent circuit of spiral resonators and coupling model is shown in Fig. 1(b) basing on [17] and Fig. 2. L and C are the self-inductance and self-capacitance while the C_m and L_m are the mutual-capacitance
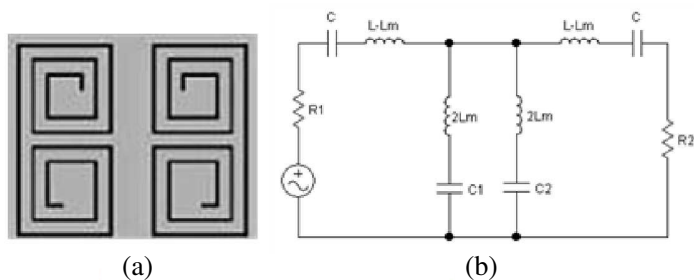
Figure 1. (a) The spiral resonators structure. (b) The equivalent circuit of spiral resonators and mixed coupling model.

Figure 2. The coupling model for the spiral resonators based on E field and H field theory.

and mutual-inductance respectively. Meanwhile, f_{ee} and f_{me} are the resonant frequencies for the circuit models in Fig. 4 and Fig. 3 respectively when the the symmetry plane T-T' is replaced by an electric wall (or a short-circuit). f_{em} and f_{mm} are also the resonant frequencies for the circuit models in Fig. 4 and Fig. 3 respectively when the plane T-T' is replaced by an magnetic wall (or an open-circuit). As is shown in Fig. 2 that the electric coupling and magnetic coupling are actually the electric field energy and magnetic energy respectively stimulated by the interaction between two resonators. Furthermore, the k_e and k_m can be defined as proportion for the stimulated electric energy in total electric energy and proportion for the stimulated magnetic energy in total magnetic energy respectively proposed in Fig. 2.
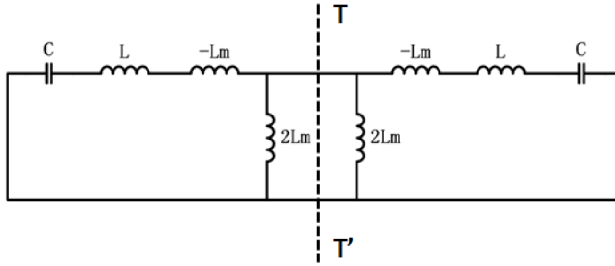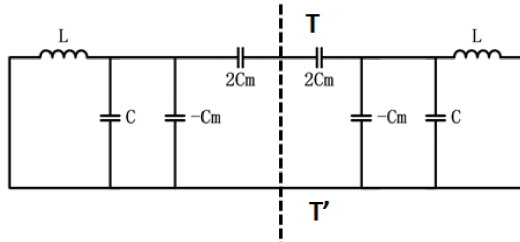
Figure 3. The magnetic coupling model.

Figure 4. The electric coupling model.

For the electric coupling model, the method to calculate the electric coupling coefficient can be as follows:

$$f_{em} = \frac{1}{2\Pi\sqrt{L(C - C_m)}}. \tag{1}$$

$$f_{ee} = \frac{1}{2\Pi\sqrt{L(C + C_m)}}. \tag{2}$$

$$k_e = \frac{(f_{em})^2 - (f_{ee})^2}{(f_{em})^2 + (f_{ee})^2} = \frac{C_m}{C} \tag{3}$$

For the magnetic coupling model, the method to calculate the magnetic coupling coefficient can be as follows:

$$f_{me} = \frac{1}{2\Pi\sqrt{C(L - L_m)}}. \tag{4}$$

$$f_{mm} = \frac{1}{2\Pi\sqrt{C(L + L_m)}}. \tag{5}$$

$$k_m = \frac{(f_{me})^2 - (f_{mm})^2}{(f_{me})^2 + (f_{mm})^2} = \frac{L_m}{L}. \tag{6}$$

For the mixed coupling model, the equations to compute the mixed coupling coefficient can be as follows:

$$\omega_{odd} = \sqrt{\frac{C_m - C}{(L + L_m)CC_m}}. \tag{7}$$

$$f_z = f_0\sqrt{\frac{k_e}{k_m}}. \tag{8}$$

$$\omega_{even} = \sqrt{\frac{C_m + C}{(L + L_m)CC_m}}. \tag{9}$$

$$C_1 = \frac{CC_m}{C_m - C}. \tag{10}$$

$$C_2 = \frac{C_m}{2}. \tag{11}$$

$$k = \frac{(\omega_{odd})^2 - (\omega_{even})^2}{(\omega_{odd})^2 + (\omega_{even})^2} = \frac{k_m - k_e}{1 - k_m k_e} = \frac{(f_u)^2 - (f_l)^2}{(f_u)^2 + (f_l)^2}. \tag{12}$$

ω_{even} is even mode resonant frequency, ω_{odd} is the odd mode frequency. f_u and f_l stand for the two simulated resonant frequencies for the spiral resonators simulated in IE3D respectively, f_z is the transmission zero frequency most adjacent to f_0. The mixed coupling coefficient k, electric coupling coefficient k_e and magnetic coupling coefficient k_m can be deduced from the Equations (1)–(12) above.

Through using the meandering slot-lines to replace the original straight slot-line, a better k can be achieved, as shown in Fig. 6. It can be inferred that the k in Fig. 6 is bigger than that in Fig. 5 for the same x and y so that the coupling coefficient k can be enhanced if straight
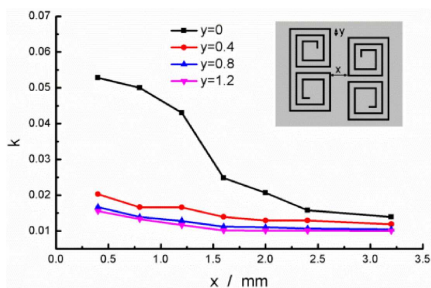

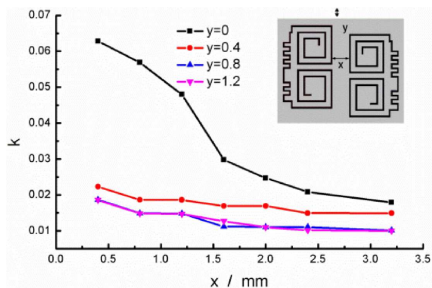**Figure 5.** The response of the coupling coefficient k for the spiral resonators.

Figure 6. The response of the coupling coefficient k for the spiral resonators with meandering slot-lines.

slot-lines in the spirals are replaced by meandering slot-lines in Fig. 6. Furthermore, the coupling coefficient k decreases with increasing of the horizontal distance x and vertical distance y, as shown in Fig. 5 and Fig. 6.

2.2. The Structure for the Spurious Response Suppression

Depending on the analysis above, the primary design of the coplanar filter was proposed, as shown in Fig. 7. The frequency response of the filter is shown as Fig. 10(a).

It can be known from Fig. 10(a) that the spurious response exist for the original coplanar filter. So the asymmetric open-stubs, rectangular micro-strip and L slot-lines are introduced, shown in Fig. 9.

The L slot-lines can generate transmission zeros near $7f_0$, $9f_0$ and $11f_0$. The frequency response of the filter is shown as Fig. 10(b) after L slot-lines were added in the original structure. Then rectangular micro-strips were further added, another transmission zero near $5f_0$
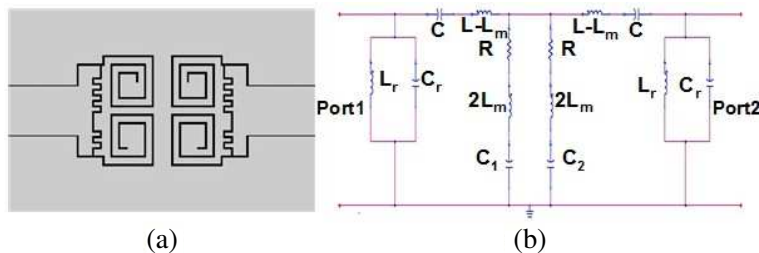

(a)   (b)

Figure 7. (a) The original coplanar filter. (b) The equivalent circuit model of the original filter.
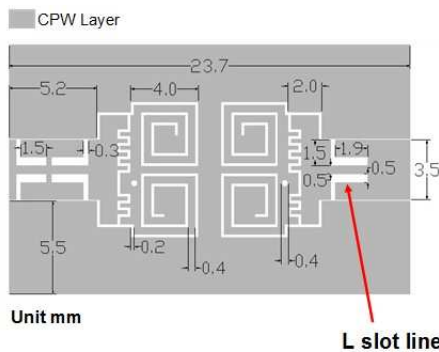

Figure 8. Top side of the novel miniaturized slot-line filter proposed in this paper ((1): The L slot lines (Unit: mm).
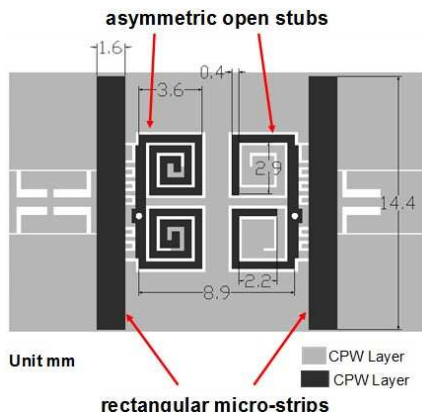
Figure 9. Bottom side of the novel filter. (1) The asymmetric open-stubs. (2) The rectangular microstrips (Unit: mm).
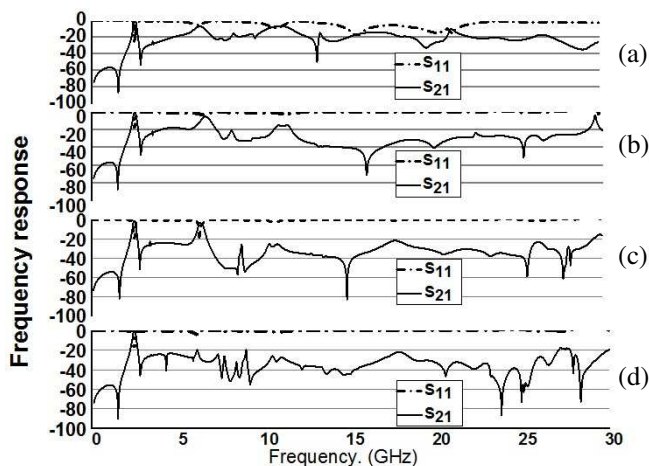
Figure 10. The simulated S_{21} frequency response in IE3D. (a) The coplanar filter in Fig. 2. (b) The coplanar filter with L slot-lines. (c) The coplanar filter with L slot-lines and rectangular micro-strips. (d) The coplanar filter with asymmetric open-stubs, rectangular micro-strip and L slot-lines (The novel filter in this paper shown in Fig. 8).

was generated, and the frequency response of the filter is shown as Fig. 10(c). When asymmetric open-stubs were finally added, the spurious response around $3f_0$ was also depressed. The final frequency response is shown as Fig. 10(d).

The equivalent circuit model of the asymmetric open-stubs, the rectangular micro-strips and the L slot-lines are presented in Fig. 11, Fig. 12 and Fig. 13. Furthermore, the simulation results obtained from ADS 2009 are given simultaneously, which verifies the feasibility of the models. The exact frequency of transmission zeros would depend on the actual dimensions and the locations of the asymmetric open-stubs, the L slot-lines and the rectangular micro-strips.

S_{21} of the asymmetric open-stub model in Fig. 11(a) can be

(a)   (b)
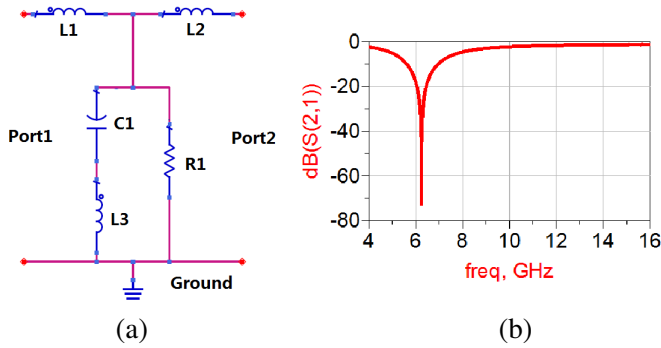
Figure 11. The model for the asymmetric open-stubs. (a) The simplified model of the asymmetric open-stubs. (b) Simulated results in ADS for the model. ($C_1 = 0.65\,\text{pF}$, $L_1 = 1\,\text{pH}$, $L_2 = 1\,\text{pH}$, $L_3 = 1\,\text{nH}$, $R_1 = 200\,\Omega$).

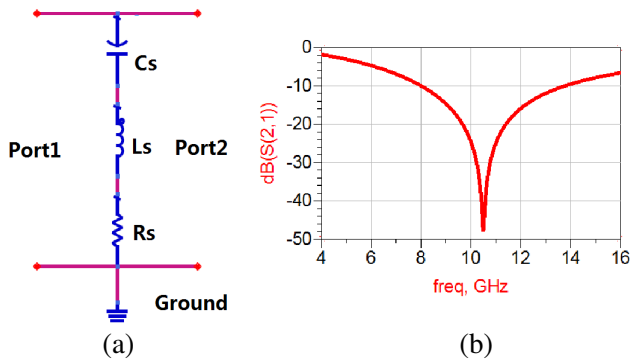(a)   (b)

Figure 12. The model for the rectangular micro-strips. (a) The simplified model of the rectangular micro-strips. (b) Simulated results in ADS for the model. ($C_S = 1\,\text{pF}$, $L_S = 230\,\text{pH}$, $R_S = 0.1\,\Omega$).
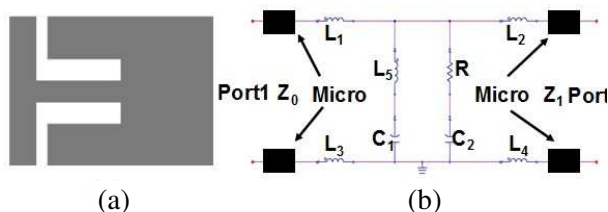
(a)   (b)

Figure 13. The simplified model of L slot-lines. (a) The L slot-line structure. (b) The circuit model of the L slot-line.

expressed as:

$$S_{21}$$

$$= \frac{2j\omega L_1 + \frac{2(1-\omega^2 C_1 L_3)R_3(j\omega L_2+Z_0)}{j\omega C_1 R_3(j\omega L_2+Z_0)+(1-\omega^2 C_1 L_3)(j\omega L_2+Z_0)+R_3(1-\omega^2 C_1 L_3)}}{Z_0 + j\omega L_1 + \frac{(1-\omega^2 C_1 L_3)R_3(j\omega L_2+Z_0)}{j\omega C_1 R_3(j\omega L_2+Z_0)+(1-\omega^2 C_1 L_3)(j\omega L_2+Z_0)+R_3(1-\omega^2 C_1 L_3)}}. \quad (13)$$

S_{21} of the rectangular micro-strips model in Fig. 12(a) can be expressed as:

$$S_{21} = \frac{j\omega R_s C_s Z_0 + Z_0 - \omega^2 L_s C_s Z_0}{j\omega \left(2 R_s C_s Z_0 + C_s (Z_0)^2\right) + 2Z_0 - 2\omega^2 L_s C_s Z_0}. \quad (14)$$

Z_0 in Equations (12) and (13) is assumed as 50.

According to the analysis above, the L slot-lines can generate transmission zeros around $7f_0$, $9f_0$ and $11f_0$ so that the harmonic responses have been suppressed successfully. The theory model for L slot-lines is shown as Fig. 13:

The micro-strip with L slot line has been represented by the model in Fig. 13(b). The change caused by the slot line may be simulated and computed approximately using the circuit model in Fig. 13.

The S_{21} expression for the model in the Fig. 14(a) is:

$$S_{21} = \frac{\left(\frac{2Z_0}{\frac{j\omega C_1}{1-\omega^2 L_5 C_1} + \frac{j\omega C_2}{1+j\omega C_2 R} + \frac{1}{j\omega(L_2+L_4)+Z_0}}\right)}{(Z_0 + j\omega L_1 + j\omega L(3))(j\omega L_2 + j\omega L_4 + Z_0)+} \quad (15)$$
$$\left(\frac{(j\omega L_2 + j\omega L_4 + Z_0)}{\frac{j\omega C_1}{1-\omega^2 L_5 C_1} + \frac{j\omega C_2}{1+j\omega C_2 R} + \frac{1}{j\omega(L_2+L_4)+Z_0}}\right)$$

As is shown in Fig. 14(b). When the value of C_1 changes ($C_1 = 0.06\,\text{pF}$, $C_1 = 0.035\,\text{pF}$, $C_1 = 0.03\,\text{pF}$), the transmission zero is at about $20\,\text{GHz}$ ($7f_0$), $26\,\text{GHz}$ ($9f_0$) and $29\,\text{GHz}$ ($11f_0$) respectively. So the simulated result of the model illustrates that the L slot-lines can create transmission zeros around $7f_0$, $9f_0$ and $11f_0$.

3. THE MEASURED RESULTS ANALYSIS

To verify the feasibility of the theory and the filter, the novel slot-line filter was implemented on a RT5870 substrate (the thickness of the substrate is 0.508 mm), as shown in Fig. 15.

The filter was tested using vector network analyzer of Rohde Schwarz ZVA40. The I/O port impedance was adjusted to 50 Ω, and the measured results shown in Figs. 16 and 17 demonstrate that the structure has a center frequency of 2.43 GHz, 3-dB passband bandwidth of 123 MHz, typical insertion loss of 24 dB, and minimum return loss of 1.75 dB.

The stop-band has been extended to 30 GHz. The simulation results from ADS 2009 and IE3D are given simultaneously, which show a good accordance with the experimental data. Besides, the size is miniaturized to 23.7 mm ∗ 14.725 mm (about $0.152\lambda ∗ 0.103\lambda$, where λ is the wavelength at 2.43 GHz in this paper).

The external quality factor (Q_E) of the proposed filter can be

(a)   (b)

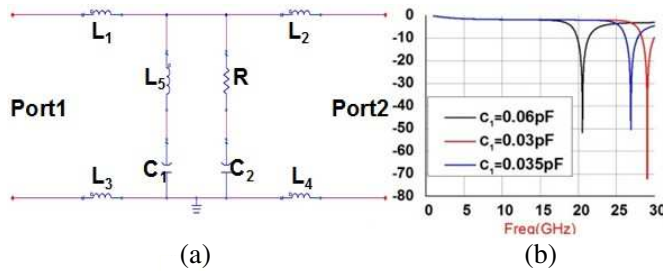**Figure 14.** The two port network for the circuit model of the L slot-line and the simulated result in ADS. (a) The two port network for the circuit model of the L slot-line. (b) The simulated results in ADS ($L_1 = L_2 = L_3 = L_4 = 0.05$ nH, $L_5 = 1$ nH, $R = 100\,\Omega$, $C_2 = 0.5$ pF).

(a)   (b)
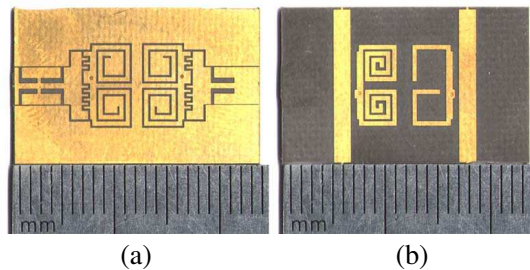
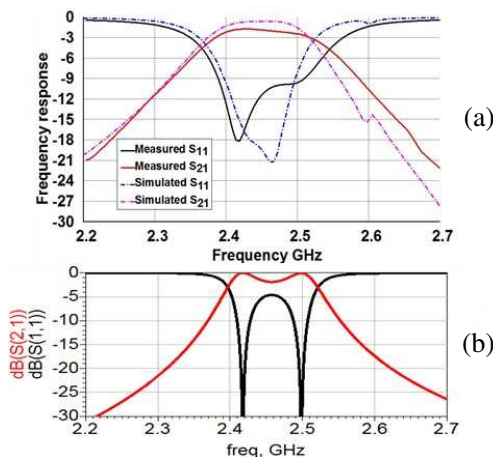**Figure 15.** The fabricated filter. (a) Top side. (b) Bottom side.

Figure 16. The simulated and measured passbands. (a) The simulated(in IE3D) and measured frequency responses for passband. (b) The simulated passband in ADS 2009 based on the equivalent circuit in Fig. 4(b) (parameters of the components are given as: $C_r = 63\,\text{pF}$, $L_r = 63\,\text{pH}$, $L - L_m = 19.2474\,\text{pH}$, $R = 0.5\,\text{ohm}$, $2L_m = 1.979\,\text{pH}$, $C = 6\,\text{pF}$, $C_1 = 1.58\,\text{pF}$, $C_2 = 1\,\text{pF}$). (c) The measured passband response.
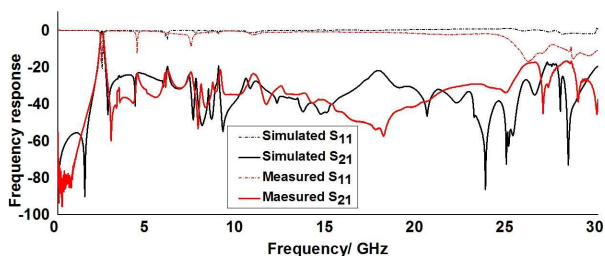
Figure 17. Frequency responses of the measured and simulated (IE3D) results for the whole frequency band.

calculated as follows:

$$Q_E = \frac{f_0}{\Delta f_{\pm 90°}}. \tag{16}$$

where $\Delta f_{90°}$ is the bandwidth at which the phase of the S_{11} response shifts $90°$ with respect to the absolute phase of the center resonance f_0. In this paper Q_E is about 29.6. The Table below gives the comparison between our work and recently reported bandpass filters with wide-stopband.

Table 1. Some references comparison.

Ref.	Size	stopband	center frequency	Q
1	about 40 mm * 35 mm	to 3.8 GHz	2.4 GHz	–
3	about 25.2 mm * 24.5 mm	to 12 GHz	5 GHz	–
11	about 56 mm * 56 mm	to 13 GHz	1.52 GHz	21.1
12	about 73 mm * 20 mm	to 10 GHz	1.5 GHz	–
13	about 80 mm * 68 mm	to 25 GHz	12 GHz	–
14	55 mm * 24.1 mm	to 20 GHz	2.25 GHz	5.65
15	30 mm * 30 mm	to 7 GHz	2.7 GHz	–
16	24 mm * 24 mm	to 16 GHz	2.44 GHz	24.4
21	about 1000 mm * 30 mm	to 8 GHz	2.4 GHz	–
23	39.8 mm * 46.4 mm	to 20 GHz	1.55 GHz	–
24	about 56 mm * 60 mm	to 10 GHz	2.3 GHz	15.3
25	about 110 mm * 10 mm	to 13 GHz	1.5 GHz	11.47
26	56 mm * 56 mm	to 8 GHz	1.5 GHz	21.1
This paper	23.7 mm * 14.7 mm	to 30 GHz	2.43 GHz	29.6

4. CONCLUSION

In this paper, a novel miniaturized slot-line filter with a stop-band up to 30 GHz has been fabricated. The spurious responses around $3f_0$, $5f_0$, $7f_0$, $9f_0$ and $11f_0$ disappeared so that this filter with a 3 dB bandwidth of 123 MHz and a center frequency of 2.43 GHz can be applied to blue-tooth technology. The rectangular micro-strips proposed to give a great suppression around $5f_0$ is analyzed in detail through the equivalent circuit as well as the asymmetric open-stubs that can create a transmission zero around $3f_0$ to suppress the spurious response. Furthermore, the outstanding performance is achieved in the

compact size of $23.7\,\mathrm{mm} * 14.725\,\mathrm{mm}$ ($0.152\lambda * 0.103\lambda$). According to the simulated and measured results above, we can demonstrate that the novel filter and the equivalent circuit model theory are feasible.

REFERENCES

1. Mo, S.-G., Z.-Y. Yu, and L. Zhang, "Design of triple-mode bandpass Filter using improved hexagonal loop resonator," *Progress In Electromagnetics Research*, Vol. 96, 117–125, 2009.

2. Coudos, S. K., Z. D. Zaharis, and T. V. Yioultsis, "Application of a differential evolution algorithm with strategy adaptation to the design of multi-band microwave filters for wireless communications," *Progress In Electromagnetics Research*, Vol. 109, 123–137, 2010.

3. Wu, L.-S., J.-F. Mao, W. Shen, and W.-Y. Yin, "Extended doublet bandpass filters implemented with microstrip resonator and full-/half-mode substrate integrated cavities," *Progress In Electromagnetics Research*, Vol. 108, 433–447, 2010.

4. Chiou, Y.-C., P.-S. Yang, J.-T. Kuo, and C.-Y.Wu, "Transmission zero design graph for dual-mode dual-band filter with periodic stepped-impedance ring resonator," *Progress In Electromagnetics Research*, Vol. 108, 23–36, 2010.

5. Wang, X.-H., B.-Z. Wang, and K. J. Chen, "Compact broadband dual-band bandpass Filters using slotted ground structures," *Progress In Electromagnetics Research*, Vol. 82, 151–166, 2008.

6. Wen, C.-P., "Coplanar waveguide, a surface strip transmission line suitable for nonreciprocal gyromacnetic device applications," *Microwave Symposium, G-MTT International*, 110–115, 1969.

7. Wada, K. and I. Awai, "Heuristic models of half-wavelength resonator bandpass filter with attenuation poles," *Electronics Letters*, Vol. 35, No. 5, 401–402, Mar. 1999.

8. William, D. F. and S. E. Schwarz, "Design and performance of coplanar waveguide bandpass filters," *IEEE Trans. on Microwave Theory and Tech.*, Vol. 31, No. 7, 558–566, Mar. 1983.

9. Sanada, A., H. Takehara, and I. Awai, "Design of the CPW in-line $\lambda/4$ stepped-impedance resonator bandpass filter," *Asia-Pacific Microwave Conference Proceedings, APMC*, Vol. 2, 633–636, 2001.

10. Lin, S.-C., T.-N. Kuo, Y.-S. Lin, and C.-H. Chen, "Novel coplanar-waveguide bandpass filters using loaded air-bridge enhanced capacitors and broadside-coupled transition structures for wideband spurious suppression," *IEEE Trans. on Microwave Theory and Tech.*, Vol. 54, No. 8, 3359–3369, Aug. 2006.

11. Chen, C.-F., T.-Y. Huang, and R.-B. Wu, "Design of microstrip bandpass filters with multi-order spurious-mode suppression," *IEEE Trans. on Microwave Theory and Tech.*, Vol. 53, No. 12, 3788–3793, Dec. 2005.

12. Kuo, J.-T. and E. Shih, "Microstrip stepped impedance resonator bandpass filter with an extended optimal rejection bandwidth," *IEEE Trans. on Microwave Theory and Tech.*, Vol. 51, No. 5, 1554–1559, May 2003.

13. Kim, I., N. Kingsley, M. Morton, R. Bairavasubramanian, J. Papapolymerou, M.-M. Tentzeris, and J.-G. Yook, "Fractal-shaped microstrip coupled-line bandpass filters for suppression of second harmonic," *IEEE Trans. on Microwave Theory and Tech.*, Vol. 53, No. 9, 2943–2948, Sep. 2005.

14. Luo, X., J.-G. Ma, and E.-P. Li, "Bandpass filter with wide stopband using broadside-coupled microstrip T-stub/DGS cell," *Microwave and Optical Technology Letters.*, Vol. 53, No. 8, 1786–1789, Aug. 2011.

15. Wang, L. G. and L. Jin, "A quasi-elliptic microstrip bandpass filter using modified anti-parallel coupled-line," *Progress In Electromagnetics Research*, Vol. 138, 245–253, 2013.

16. Luo, X. and J.-G. Ma, "Compact slot-line bandpass filter using backside microstrip open-stubs and air-bridge structure for spurious suppression," *Asia-Pacific Microwave Conference Proceedings, APMC*, 882–885, 2009.

17. Hong, J.-S. and M.-J. Lancaster, "Couplings of microstrip square II open-loop resonators for cross-coupled planar microwave filters," *IEEE Trans. on Microwave Theory and Tech.*, Vol. 44, No. 12, 2099–2109, Dec. 1996.

18. Wu, Y.-L., C. Liao, and X.-Z. Xiong "A dual-wideband bandpass filter based on E-shaped microstrip sir with improved upper-stopband performance," *Progress In Electromagnetics Research*, Vol. 108, 141–153, 2010.

19. Kuo, J.-T., C.-Y. Fan, and S.-C. Tang "Dual-wideband bandpass filters with extended stopband based on coupled-line and coupled three-line resonators," *Progress In Electromagnetics Research*, Vol. 124, 1–15, 2012.

20. Mashhadi, M. and N. Komjani, "Design of dual-band bandpass filter with wide upper stopband using sir and GSIR structures," *Progress In Electromagnetics Research*, Vol. 32, 221–232, 2012.

21. Tiwary, A. K. and N. Gupta, "Design of compact coupled microstrip line band pass filter with improved stopband characteristics," *Progress In Electromagnetics Research*, Vol. 24,

97–109, 2011.

22. Lin, W.-J., C.-S. Chang, and J.-Y. Li, "Improved compact broadband bandpass filter using branch stubs co-via structure with wide stopband characteristics," *Progress In Electromagnetics Research*, Vol. 5, 45–55, 2008.

23. Lin, S.-C. and C.-Y. Yeh, "stopband-extented balanced filters using both $\lambda/4$ and $\lambda/2$ sirs with common-mode suppression and improved passband selectivity," *Progress In Electromagnetics Research*, Vol. 128, 215–228, 2012.

24. Kim, C.-S., D.-H. Kim, I.-S. Song, K. M. K. H. Leong, T. Itoh, and D. Ahn, "A design of a ring bandpass filters with wide rejection band using DGS and spur-line coupling structures," *IEEE MTT-S International Microwave Symposium*, Vol. 128, 2183–2186, 2005.

25. Kuo, J.-T. and E. Shih, "Microstrip stepped impedance resonator bandpass filter with an extended optimal rejection bandwidth," *IEEE Trans. on Microwave Theory and Tech.*, Vol. 51, 1554–1559, 2003.

26. Chen, C.-F., T.-Y. Huang, and R.-B. Wu, "Design of microstrip bandpass filters with multiorder spurious-mode suppression," *IEEE Trans. on Microwave Theory and Tech.*, Vol. 53, 3788–3793, 2005.